



## Solution structure of the N-terminal transactivation domain of ERM modified by SUMO-1

Zoé Lens<sup>a,c</sup>, Frédérique Dewitte<sup>a</sup>, Didier Monté<sup>a</sup>, Jean-Luc Baert<sup>a</sup>, Coralie Bompard<sup>a</sup>, Magalie Sénéchal<sup>b</sup>, Carine Van Lint<sup>c</sup>, Yvan de Launoit<sup>b</sup>, Vincent Villeret<sup>a,\*</sup>, Alexis Verger<sup>a,\*\*</sup>

<sup>a</sup> IRI USR 3078 CNRS, Parc CNRS de la Haute Borne, 50 Avenue de Halley, BP 70478, 59658 Villeneuve d'Ascq Cedex, France

<sup>b</sup> IBL UMR 8161 CNRS, 1 Rue du Professeur Calmette, Lille 59021, France

<sup>c</sup> Institut de Biologie et de Médecine Moléculaires (IBMM), Université Libre de Bruxelles, Rue des Professeurs Jeener et Brachet 12, 6041 Gosselies, Belgium

### ARTICLE INFO

#### Article history:

Received 7 July 2010

Available online 18 July 2010

#### Keywords:

SAXS

ERM

SUMO

Transactivation domain

Intrinsically disordered

### ABSTRACT

ERM is a member of the PEA3 group of the Ets transcription factor family that plays important roles in development and tumorigenesis. The PEA3s share an N-terminal transactivation domain (TADn) whose activity is inhibited by small ubiquitin-like modifier (SUMO). However, the consequences of sumoylation and its underlying molecular mechanism remain unclear. The domain structure of ERM TADn alone or modified by SUMO-1 was analyzed using small-angle X-ray scattering (SAXS). Low resolution shapes determined *ab initio* from the scattering data indicated an elongated shape and an unstructured conformation of TADn in solution. Covalent attachment of SUMO-1 does not perturb the structure of TADn as indicated by the linear arrangement of the SUMO moiety with respect to TADn. Thus, ERM belongs to the growing family of proteins that contain intrinsically unstructured regions. The flexible nature of TADn may be instrumental for ERM recognition and binding to diverse molecular partners.

© 2010 Elsevier Inc. All rights reserved.

### 1. Introduction

Transcription factors are modular entities usually built up with distinct and separable domains dedicated to DNA-binding and transcriptional regulation. Whereas DNA-binding domains fall into a relatively small number of clearly defined structural categories, activation (TAD) and repression domains have proved to be significantly more diverse and it can be argued that they have defied classification. Relatively sophisticated structures are required to distinguish one DNA sequence from another, but it appears that much simpler motifs suffice for the protein–protein interactions that underlie gene activation and repression [1].

Accordingly, it appears that most activation and repression domains do not have any permanent tertiary structure but consist of a series of very short motifs that dock with partners, and sometimes only adopt structure during the binding process [2]. Consistent with this view, little progress has been made defining the three dimensional structures of activation and repression domains. One of the most extensively studied activators are those that contain acidic transcriptional activation domain and two highly investigated acidic activators are the human tumor suppressor p53 and

the Herpes Simplex Virion protein 16 (VP16) [3,4]. It has been shown that their TADs are mostly devoid of regular secondary structure elements in their free state and that they become more ordered when bound to their target proteins, adopting a short alpha-helical conformation that has specificity to its targets [3,4].

ERM [5], PEA3 and ER81 belong to the PEA3 sub-family of Ets transcription factors [6]. They share the highly conserved ETS DNA-binding domain and two conserved transcriptional activation domains, one located at the amino-terminus (TADn) and the other at the carboxy-terminus (TADc) (Fig. 1A) [6]. In particular, TADn is an acidic TAD which contains a 20 amino acid stretch predicted to form an alpha-helix while the rest of TADn may be intrinsically disordered [7–9], reminiscent of the p53 and VP16 TADs. Moreover, we have recently shown that the activity of TADn is inhibited by a flanking domain named the negative regulatory domain (NRD) (Fig. 1A). The NRD domain contains three SUMO sites, one of which being in the overlapping segment with TADn on lysine 89 [10,11]. How the conformation of TADn allows the recruitment of partners and how sumoylation may influence its activity has still to be unraveled.

Intrinsically disordered proteins (IDP) are frequently involved in key biological processes such as cell cycle control, transcriptional regulation and signal transduction [12]. An intrinsically disordered protein or domain is likely a key structural feature that facilitates binding to many partners and is also accessible for post-translational modifications. Therefore, their structural characterization cannot be achieved solely by diffraction techniques but requires the use of

\* Corresponding author. Fax: +33 3 62 53 17 01.

\*\* Corresponding author. Fax: +33 3 62 53 17 01.

E-mail addresses: [vincent.villeret@iri.univ-lille1.fr](mailto:vincent.villeret@iri.univ-lille1.fr) (V. Villeret), [alexis.verger@iri.univ-lille1.fr](mailto:alexis.verger@iri.univ-lille1.fr) (A. Verger).

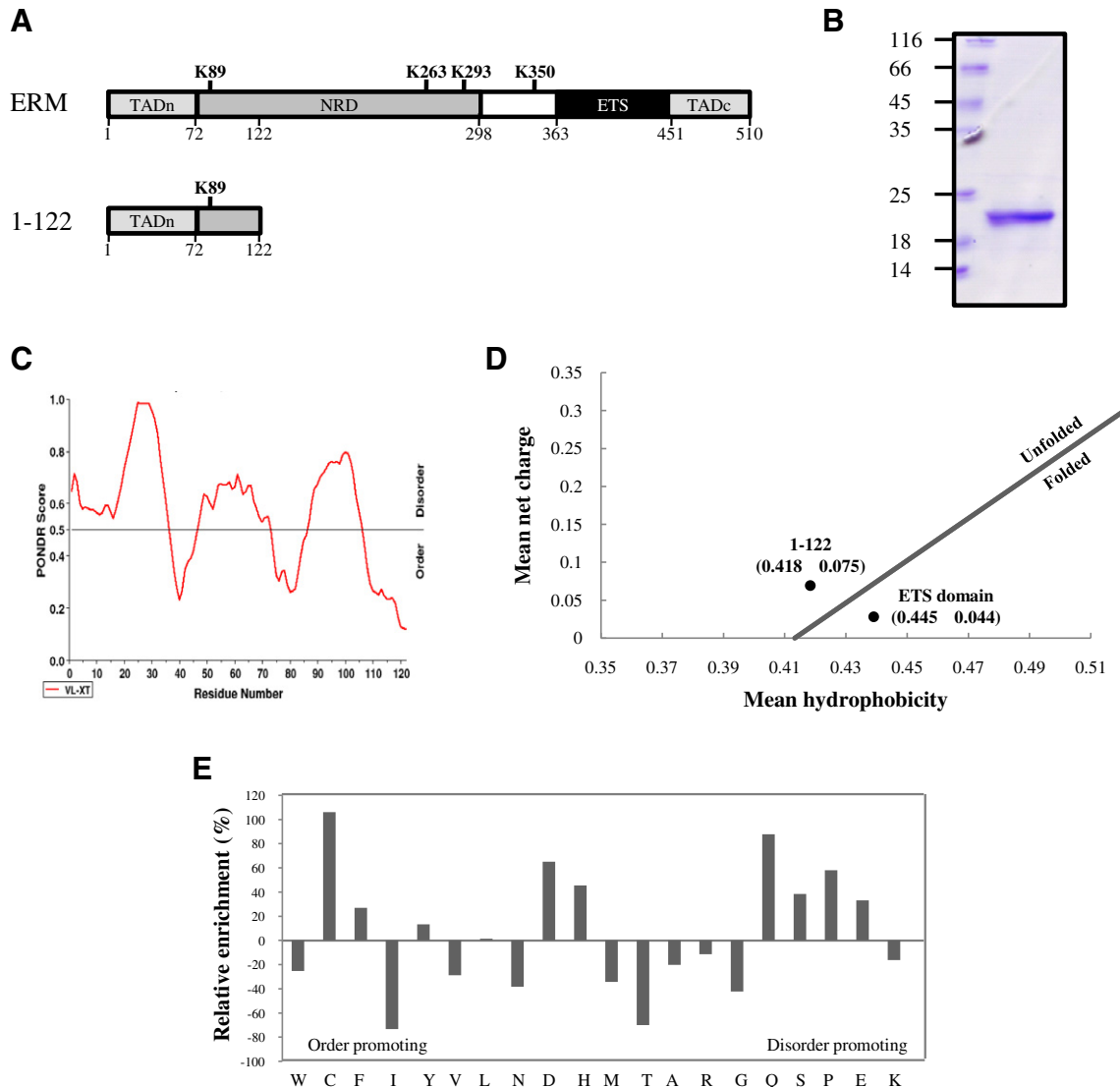


**Fig. 1.** The N-terminal transactivation domain (TADn) of ERM is intrinsically unstructured. (A) Schematic diagrams of ERM full-length and ERM TADn. The N-terminal transactivation domain (TADn), the negative regulatory domain (NRD) and the ETS DNA-binding domain (ETS) are shown in shaded boxes. The four SUMO sites are indicated. (B) SDS/PAGE (15% gel) of purified His<sub>6</sub>-TADn. Molecular mass (kDa) is indicated. (C) Primary sequence analyzed with PONDR indicates that ERM TADn is a mostly disordered protein with three short ordered regions. (D) Natively folded and unfolded proteins/domains are separated by a linear boundary, which is described by the following relationship:  $H_b = (R + 1.151)/2.785$ , where  $H_b$  is the boundary mean hydrophobicity value and  $R$  mean net charge according to [16]. (E) Deviations in amino acid composition of ERM TADn from the average values in the SWISS-PROT database. The relative enrichment of order-promoting and disorder-promoting residues is illustrated.

other solution methods. SAXS is a powerful technique that allows the determination of molecular shape at low resolution and is well suited for the study of partially folded proteins in solution [13].

In this study, we used low resolution approach to characterize for the first time the structural properties of the N-terminal transactivation domain of ERM alone or modified by SUMO-1 on K89. Together with theoretical prediction, all experiments support the hypothesis that ERM belongs to the growing class of the intrinsically disordered proteins. Our SAXS study reveals an extended and flexible conformation for TADn and suggests that the covalent attachment of SUMO-1 does not perturb its structural flexibility.

## 2. Materials and methods

### 2.1. Plasmid constructs

The cDNA encoding the N-terminal transactivation domain of human ERM (residues 1–122) was amplified by PCR using pSV-

ERM as template and appropriate oligonucleotides. Detailed primer information is available upon request. The amplified cDNA was digested with *Nco*I and *Xho*I and was ligated into the pET24d vector. pT-E1E2S1 has been described [14] and was kindly provided by Saitoh and co-workers.

### 2.2. Protein purification

*Escherichia coli* strain BL21 (DE3) was transformed with pET24d-ERM TADn and pT-E1E2S1 and grown at 37 °C in LB medium (4 l) containing 25 µg/ml Kanamycin and 25 µg/ml Chloramphenicol until the OD<sub>600</sub> reached 0.8. Co-expression of TADn, E1, E2 enzymes and SUMO-1 protein was induced by the addition of 0.1 mM IPTG at 37 °C. After a 4 h culture, the cells were harvested by centrifugation and stored frozen at –20 °C. Frozen cell pellets were resuspended in lysis buffer containing 50 mM Hepes, pH 8.0, 200 mM NaCl, 1 mM DTT, 5 mM imidazole supplemented with Complete EDTA-free inhibitor cocktail (Roche) and DNase. The cells were disrupted by

sonication and the lysate was clarified by centrifugation at 12,000g for 40 min at 4 °C.

The supernatant was filtered using a MILLEX-HV PVDF 0.45 µm filter and was loaded onto a 5 ml Ni<sup>2+</sup>-NTA affinity chromatography superflow cartridge (Qiagen) pre-equilibrated with 10 volumes of lysis buffer. TADn alone and TADn modified by SUMO-1 were eluted with buffer containing 50 mM Hepes, pH 8.0, 200 mM NaCl, 1 mM DTT and 250 mM imidazole. Fractions were next loaded onto a 1 ml MonoQ HR 5/5 column (GE Healthcare) and eluted using a linear gradient of NaCl (from 0.1 to 1.0 M). Fractions containing TADn alone and those enriched in sumoylated TADn were further purified onto a gel-filtration HiLoad 16/60 Superdex 75 column (GE Healthcare) in final buffer containing 50 mM Hepes, pH 8.0, 200 mM NaCl, 1 mM DTT and 5% glycerol. Protein samples were then concentrated and stored at –20 °C. Proteins were analyzed by Coomassie Brilliant Blue staining and Western blot.

### 2.3. Western blot

Ten micrograms of purified TADn and TADn-SUMO-1 were separated by SDS-PAGE on a 15% poly-acrylamide gel and transferred onto nitrocellulose membrane at 60 V overnight at 4 °C. The membrane was washed once in 50 mM Tris/HCl, pH 7.5, containing 150 mM NaCl and 0.05% Tween-20 (Tris/NaCl/Tween), then incubated at room temperature in skimmed milk powder solution [5% (w/v) in Tris/NaCl/Tween] for 1 h. The membrane was rinsed in Tris/NaCl/Tween and incubated for 1 h with gentle shaking in 10 ml Tris/NaCl/Tween containing 10 µg of primary antibody. After five washes with 150 ml Tris/NaCl/Tween, the secondary antibody solution was added and incubation was continued for 1 h. The membrane was washed for 1 h in several changes of Tris/NaCl/Tween. Detection was carried out using the Renaissance<sup>®</sup> Chemiluminescence reagent plus (NEN Life Sciences). Anti-SUMO-1 (anti-GMP-1) monoclonal antibody was provided by Zymed Laboratories.

### 2.4. Sequence analysis

Ordered and disordered regions in ERM TADn were analyzed by the PONDR<sup>®</sup> algorithm [15]. Charge-hydrophobicity plot was generated as described by Uversky [16]. Ordered and disordered domains are separated by a linear boundary with disordered domains above the boundary and ordered domains below. The hydrophobicity of each amino acid sequence was calculated by Kyte and Doolittle approximation. The hydrophobicity of individual residues was normalized to a scale of 0 to 1 for the calculations. The mean hydrophobicity ( $H_b$ ) is defined as the sum of the normalized hydrophobicities of all residues divided by the number of residues in the sequence. The mean net charge ( $R$ ) is defined as the charge of the protein divided by the number of the residues in the sequence and was calculated with Protein calculator v3.3. Deviations in the amino acid compositions of ERM TADn were calculated using the average amino acid frequencies of the SWISS-PROT database as reference values.

### 2.5. SAXS experiments

SAXS experiments were performed at the ID14EH3 beamline of the European Synchrotron Radiation Facility (Grenoble, France). Measurements were performed at 20 °C with a monochromatic X-ray beam (wavelength of  $\lambda = 1.0$  Å). The sample-to-detector distance was 1500 mm, corresponding to the scattering vector range of  $0.007 < q < 0.386$  Å<sup>–1</sup>, where  $q$  is the magnitude of the  $q$ -vector defined by  $q = (4\pi/\lambda) \sin \theta$  ( $\theta$  is the scattering angle). Buffer and sample were collected alternatively (10 successive frames of 15 s in length). For each sample, data were collected at several different protein concentrations (ERM TADn: 9.66 mg/ml, 7.19, 5.09, 2.61

and 1.59; ERM TADn modified by SUMO-1: 4.43 mg/ml, 3.38, 2.17 and 1.22) and the corresponding buffer scatterings were subtracted from every sample intensity curve.

Data were processed using standard procedures by PRIMUS [17]. The Guinier approximation  $I(q) = I(0) \exp(-q^2 R_g^2/3)$  for  $qR_g < 1$ , was used for the evaluation of the radius of gyration ( $R_g$ ).  $R_g$  was also evaluated from the pair distance distribution function  $P(r)$  which was calculated using the indirect transform package GNOM [18]. The  $P(r)$  function allowed the estimation of the maximum dimension  $D_{max}$  of the scattering molecules. A Kratky plot ( $(qR_g)^2 I(q)/I(0)$  versus  $qR_g$ ) is also represented.

Low-resolution models of ERM TADn alone or modified by SUMO-1 were generated using the program GASBOR [19]. Several independent calculations were performed and the models were averaged using the DAMAVER program suite [20]. The filtered average model is presented. Moreover, three representative models with the lowest Normalized Spatial Discrepancy (NSD) were selected and presented.

## 3. Results

### 3.1. Sequence analysis shows the disordered nature of ERM TADn

TADn of ERM (Fig. 1A) is sufficient to activate transcription and contains the first residue modified by SUMO-1 (K89), able to influence TADn activity [7,8,10,11], yet very poorly characterized structurally. Early structure predictions and circular dichroism spectrum analysis have indicated that TADn is mostly devoid of regular secondary structure elements except for the presence of a putative alpha-helix [7,9]. Purified ERM TADn (1–122) in bacteria displays an apparent molecular mass of ~20 kDa (Fig. 1B), in comparison to a theoretical molecular mass of 14 kDa. The abnormal migration might reflect its amino acid composition bias and extended conformation. Analysis of the primary sequence of TADn with the VL-XT PONDR predictor of naturally disordered regions [15] indicates a disordered tendency in most regions of TADn, with the exception of three discrete regions (Fig. 1C). A further bio-informatic analysis was carried out to check whether the N-terminal domain of ERM shows a combination of low mean hydrophobicity, compared to the boundary hydrophobicity, coupled to a relatively high net charge, as typically found in natively unfolded proteins or domains [16]. When plotting mean hydrophobicity against mean net charge for ERM 1–122, it can be seen that the amino acid composition of this N-terminal region is located within the natively unfolded protein domain (Fig. 1D). Interestingly, as positive control, the ETS DNA-binding domain of ERM is found within the natively folded protein domain. It has been shown that disordered proteins sequences are depleted in order-promoting (W, C, F, I, Y, V and L) and enriched in disorder-promoting amino acids (R, G, Q, S, P, E and K) [16]. Not surprisingly, ERM TADn showed an overall tendency to lack order-promoting residues and be enriched in disorder-promoting residues, except with respect to Cys, Phe, Gly and Lys (Fig. 1E). In combination, all of these bio-informatics tools indicate that ERM 1–122 possesses the typical amino acid composition and properties of intrinsically unstructured proteins [2,16].

### 3.2. Solution structure of ERM TADn

SAXS is a valuable technique for the study of flexible, low compactness macromolecules in solution, which has already been successfully used to characterize other intrinsically unstructured proteins [21–23]. SAXS provides important parameters like the overall size and shape of the macromolecules in solution [13].

The scattering profile of ERM TADn was obtained as described in Section 2. The Kratky plot ( $(qR_g)^2 I(q)/I(0)$  versus  $qR_g$ ) displays no trace of the bell shape associated with compact, globular particles

(Fig. 2A). Instead, the absence of a maximum in the plot and the slightly increase in the large  $q$  range suggest that TADn possesses flexible chains and may not have a well packed core. Analysis of the curve in the low  $q$  region with the Guinier approximation gave a radius of gyration ( $R_g$ ) of  $39.6 \pm 0.7$  Å. In close agreement, the distances distribution function  $P(r)$  inferred from the scattering curve (Fig. 2B) exhibits a maximum around 40 Å and a long tail up to 140 Å ( $D_{\max}$ ). Both  $D_{\max}$  and  $R_g$  values are very large for a protein of 14 kDa molecular mass, suggestive of an extremely extended conformation.

The overall envelope of TADn was generated *ab initio* from its scattering profile using the program GASBOR [19]. Ten independent runs were performed and averaged using the DAMAVER program suite [20]. Three representative GASBOR models are displayed alongside the DAMAVER average model (Fig. 2C). Resulting models were all very similar, showing a recurring extended and disordered chain of dummy residues. Taken together, bio-informatic analysis, Kratky plot,  $P(r)$  function and low-resolution models reveal that ERM TADn has the typical characteristics of intrinsically unstructured protein.

### 3.3. Solution structure of ERM TADn modified by SUMO-1

We recently showed that TADn activity is inhibited by a flanking domain named the negative regulatory domain (NRD) (Fig. 1A) [10]. The NRD domain contains three SUMO sites, one of which being in the overlapping segment with TADn on lysine 89. As a step toward understanding how sumoylation alters the biological function of ERM TADn, we measured SAXS of SUMO-1 modified TADn to examine the possible structural consequence of this post-translational modification.

We used the bacterial system developed by Saitoh and co-workers [14] to obtain large amount of recombinant SUMO-1 modified TADn. A major band migrating at  $\sim 40$  kDa, corresponding to TADn modified with one SUMO-1 moiety, was detected by Coomassie (Fig. 3A, left panel). The presence of SUMO-1 was confirmed by mass spectrometry (data not shown) and immunoblot with anti-SUMO-1 antibody (Fig. 3A, right panel). We note that three other bands are also evident in Western blot. Based on expected molecular masses, we believe that the two fastest migrating bands correspond to the addition of two and three SUMO-1 moieties and the slowest migrating band is likely a degradation product. Nevertheless, dynamic light scattering analysis (data not shown) indicates that SUMO-1 modified TADn is monodisperse and thus suitable for further SAXS characterization.

As seen with TADn (Fig. 2A), the Kratky plot for TADn modified by SUMO-1 displays no trace of the bell shape associated with compact, globular particles (Fig. 3B). The distances distribution function  $P(r)$  inferred from the scattering curve (Fig. 3C) exhibits a maximum around 42 Å and a long tail up to 160 Å ( $D_{\max}$ ). This indicates that TADn modified by SUMO-1 has a conformation slightly more extended than TADn alone. The value of  $R_g$  determined by Guinier approximation was  $40.0 \pm 0.7$  Å, which was roughly consistent with the value estimated from the  $P(r)$ . Overall molecular envelopes were obtained for TADn-SUMO-1 using the scattering data (Fig. 3D). Several independent runs yielded various shapes with recurrent features: they were all elongated with a protuberance of always the same size at one extremity that is missing in TADn (Fig. 2C). The protuberance most likely corresponds to SUMO-1 conjugated to TADn. Consistent with this, the shape and volume of SUMO-1 [24] can well accommodate the low resolution model of TADn-SUMO-1 (Fig. 4).

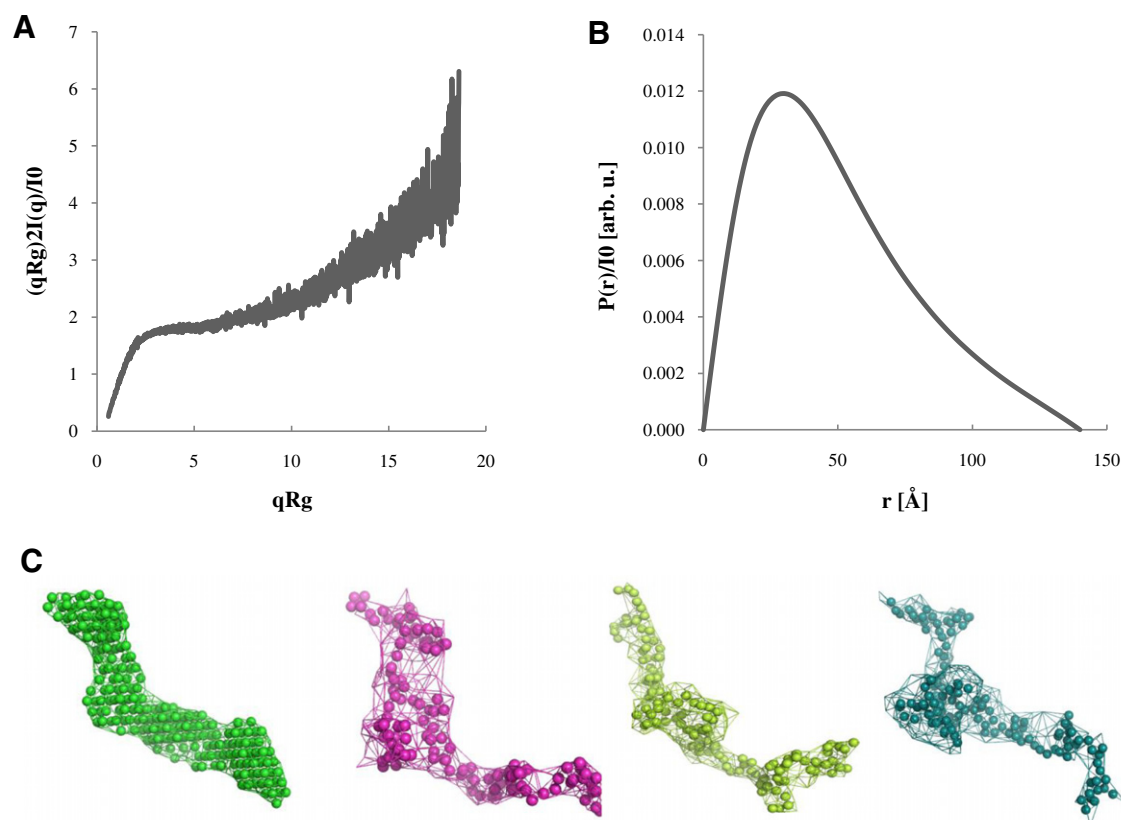


**Fig. 2.** Experimental SAXS curves and *ab initio* modeling for ERM TADn. (A) Kratky plot. (B) Pair distance distribution function  $P(r)$ . (C) Low resolution average DAMAVER model (light green) followed by three representative GASBOR models alongside. The models were displayed using the program PyMOL. (For interpretation of the references in color in this figure legend, the reader is referred to the web version of this article.)



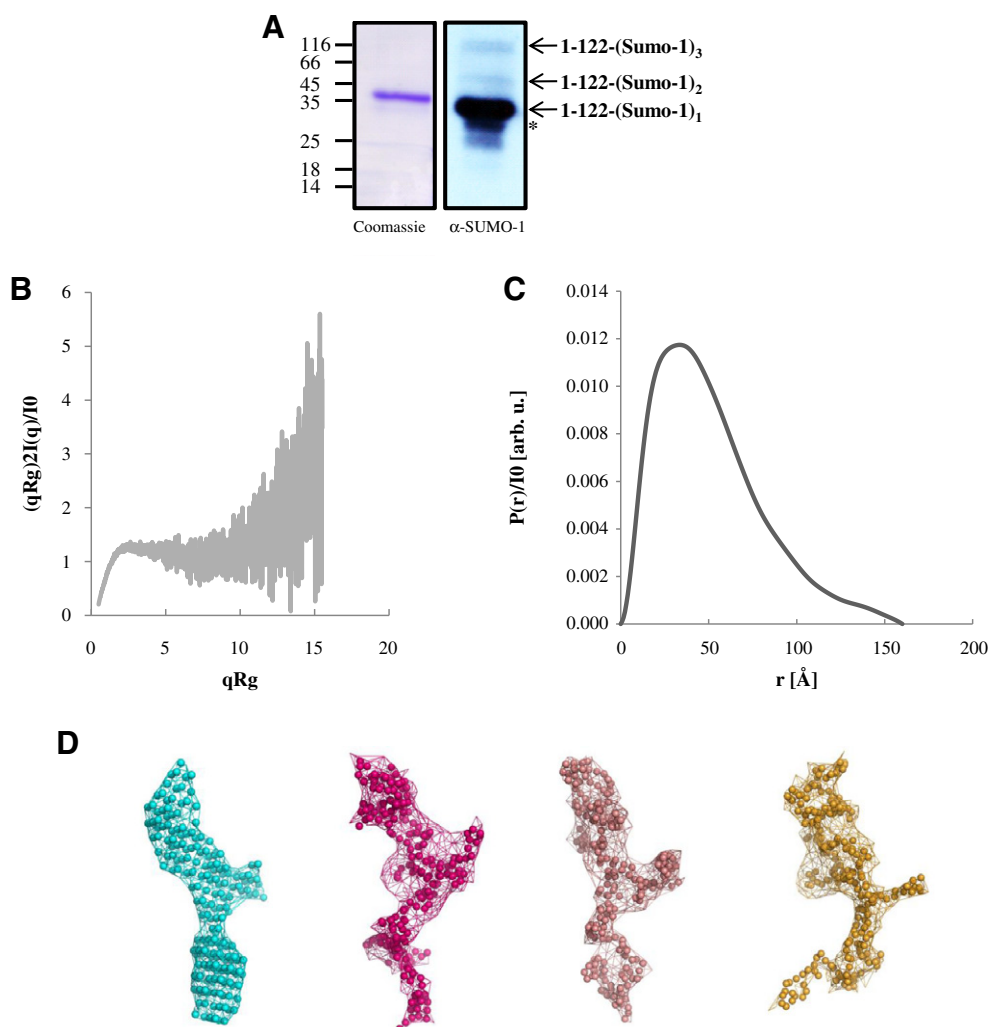


**Fig. 3.** Experimental SAXS curves and *ab initio* modeling for ERM TADn modified by SUMO-1. (A) Purified His<sub>6</sub>-TADn modified by SUMO-1 in bacteria. (Left panel) SDS/PAGE (15% gel) followed by Coomassie blue staining. (Right panel) Purified His<sub>6</sub>-TADn modified by SUMO-1 was subjected to Western blot analysis with SUMO-1 specific antibody. Thick arrows point to the covalently modified TADn. Asterisk depicts likely a degradation product. Molecular mass (kDa) is indicated. (B) Kratky plot. (C) Pair distance distribution function  $P(r)$ . (D) Low resolution average DAMAVER model (light blue) followed by three representative GASBOR models alongside. The models were displayed using the program PyMOL. (For interpretation of the references in color in this figure legend, the reader is referred to the web version of this article.)

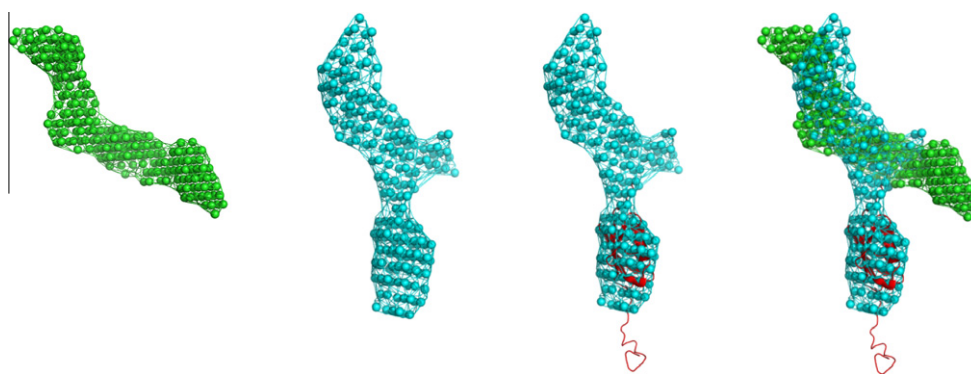


**Fig. 4.** Model of ERM TADn modified by SUMO-1. The structures of TADn, TADn-SUMO-1 and SUMO-1 are shown in green, cyan and red, respectively. The low resolution *ab initio* model of TADn-SUMO-1 obtained by DAMAVER (Fig. 3D) is superimposed to the SUMO-1 NMR solution structure (PDB code: 1A5R) [24]. (For interpretation of the references in color in this figure legend, the reader is referred to the web version of this article.)

#### 4. Discussion

In this work, we provide new information concerning the conformational properties of the N-terminal transactivation domain

of ERM in solution. The extended conformational shape determined for ERM 1–122 lead us to conclude that it is intrinsically disordered. Furthermore, by combining the low resolution structure of TADn modified by SUMO-1 with the known high resolution

structure of SUMO-1, a model for the domain arrangement was proposed. In this model (Fig. 4), no significant interactions between the two proteins beyond the region of their covalent attachment are detected. Accordingly, SUMO-1 may regulate TADn activity by acting as a structurally independent docking module, rather than through the induction of a conformational change in TADn.

Several lines of evidence have demonstrated that the N-terminal 122 amino acids of ERM are intrinsically unstructured, including the possession of primary structural features typical of disordered proteins and an elongated, non-globular shape in solution. Structural disorder has been experimentally documented in numerous TADs such as in the TAD of VP16 [4], Fos [25], p53 [26] and HY5 [27]. In fact, TADs appear to constitute an important sub-family of what is known as intrinsically disordered proteins [28]. To date, it is estimated that more than 30% of eukaryotic genomes encode contiguous unfolded regions longer than 30 amino acids in length, and up to 80% in transcription factor activation regions and cancer-associated proteins [12,28,29]. Interestingly, disordered proteins could often adopt a more ordered structure upon interaction with their partners [2]. We and others have previously shown that ERM can bind to the transcription factor Jun [30], the androgen receptor [31], the SUMO conjugating enzyme Ubc9 [11], the chromatin remodeling factor CHD3/ZFH [32] and the protein ZNF237 [33], but none of these interactions involved the first 72 N-terminal amino acid residues of ERM. Whether a specific protein partner is able to alter the conformation of TADn and thus regulate its activity remains to be determined.

Although our recent data indicate that sumoylation may modulate the transcriptional activity of ERM [10,11], the mechanism underlying this effect is not yet clear. SUMO modification can often modify the binding properties of its targets, either allowing or inhibiting protein–protein interactions. Whether this is due to conformational changes in the SUMO modified protein or due to the addition or masking of binding interfaces is still unclear. For example, the crystal structure of SUMO-1 with the thymine DNA glycosylase (TDG) revealed a well defined interface between these two proteins that appears instrumental for the release of TDG from DNA [34]. In contrast, it has been demonstrated that SUMO-1 conjugation to some targets such as Ets-1 [35], RanGAP1 [36], E2-25K [37] or HSF-2 [38] remain structurally and dynamically independent when conjugated. Consequently, for these targets, the loss or gain of interactions seems to be due to simple masking or addition of binding sites. This is exemplified by E2-25K for which SUMO modification interferes with its interaction with the ubiquitin E1 activating enzyme [37]. Consistent with these observations, we found that sumoylation of ERM (at least on the K89 residue) does not perturb the structure of TADn. However, the environment in the vicinity of ERM K89 acceptor site differs from that of previously structurally characterized SUMO targets. Whereas K89 is part of an intrinsically unstructured domain, K14 of E2-25K falls in the canonical ubiquitin conjugating enzyme E2-core fold [37], K15 of Ets-1 precedes the PNT domain [35], K82 of HSF-2 is located in the DNA-binding domain [38] and K526 of RanGAP1 is part of an extended loop structure [36]. Our finding that sumoylation of ERM occurs within intrinsically disordered region, together with observation that flexible regulatory regions of C/EBP [39] and CtBP [23] are targeted for sumoylation, suggests that sumoylation may commonly occur within IDPs.

## Acknowledgments

We would like to thank H. Saitoh for its generous gift of reagents. Z.L. is the recipient of FRIA grant (FNRS, Belgium). This work was supported by the 'Fondation pour le Recherche Médicale' (FRM, Comité Nord-Pas de Calais, France), the 'Association pour le Recherche contre le Cancer' (ARC, France), the 'Ligue Nationale contre le Cancer'

(Comité Nord, France), the Ministry of Higher Education and Research and the Nord-Pas de Calais Regional Council and FEDER through the 'Contrat de Projets Etat Région (CPER) 2007–2013'.

## References

- [1] S.J. Triezenberg, Structure and function of transcriptional activation domains, *Curr. Opin. Genet. Dev.* 5 (1995) 190–196.
- [2] H.J. Dyson, P.E. Wright, Intrinsically unstructured proteins and their functions, *Nat. Rev. Mol. Cell Biol.* 6 (2005) 197–208.
- [3] P. Di Lello, L.M. Jenkins, T.N. Jones, B.D. Nguyen, T. Hara, H. Yamaguchi, J.D. Dikeakos, E. Appella, P. Legault, J.G. Omichinski, Structure of the Tfb1/p53 complex: insights into the interaction between the p62/Tfb1 subunit of TFIIF and the activation domain of p53, *Mol. Cell* 22 (2006) 731–740.
- [4] M. Uesugi, O. Nyanguile, H. Lu, A.J. Levine, G.L. Verdine, Induced alpha helix in the VP16 activation domain upon binding to a human TAF, *Science* 277 (1997) 1310–1313.
- [5] D. Monté, J.L. Baert, P.A. Defossez, Y. de Launoit, D. Stéhelin, Molecular cloning and characterization of human ERM, a new member of the Ets family closely related to mouse PEA3 and ER81 transcription factors, *Oncogene* 9 (1994).
- [6] Y. de Launoit, J.L. Baert, A. Chotteau-Lelievre, D. Monte, L. Coutte, S. Mauen, V. Firlé, C. Degerny, K. Verreman, The Ets transcription factors of the PEA3 group: transcriptional regulators in metastasis, *Biochim. Biophys. Acta* 1766 (2006) 79–87.
- [7] P.A. Defossez, J.L. Baert, M. Monnot, Y. de Launoit, The ETS family member ERM contains an alpha-helical acidic activation domain that contacts TAFII60, *Nucleic Acids Res.* 25 (1997) 4455–4463.
- [8] M.P. Laget, P.A. Defossez, O. Albagli, J.L. Baert, F. Dewitte, D. Stéhelin, Y. de Launoit, Two functionally distinct domains responsible for transactivation by the Ets family member ERM, *Oncogene* 12 (1996) 1325–1336.
- [9] S. Mauen, I. Huvent, V. Raussens, D. Demonte, J.L. Baert, C. Tricot, J.M. Ruyschaert, C. Van Lint, N. Moguilevsky, Y. de Launoit, Expression, purification, and structural prediction of the Ets transcription factor ERM, *Biochim. Biophys. Acta* 1760 (2006) 1192–1201.
- [10] C. Degerny, Y. de Launoit, J.L. Baert, ERM transcription factor contains an inhibitory domain which functions in sumoylation-dependent manner, *Biochim. Biophys. Acta* 1779 (2008) 183–194.
- [11] C. Degerny, D. Monte, C. Beaudoin, E. Jaffray, L. Portois, R.T. Hay, Y. de Launoit, J.L. Baert, SUMO modification of the Ets-related transcription factor ERM inhibits its transcriptional activity, *J. Biol. Chem.* 280 (2005) 24330–24338.
- [12] L.M. Iakoucheva, C.J. Brown, J.D. Lawson, J. Obradovic, A.K. Dunker, Intrinsic disorder in cell-signaling and cancer-associated proteins, *J. Mol. Biol.* 323 (2002) 573–584.
- [13] C.D. Putnam, M. Hammel, G.L. Hura, J.A. Tainer, X-ray solution scattering (SAXS) combined with crystallography and computation: defining accurate macromolecular structures, conformations and assemblies in solution, *Q. Rev. Biophys.* 40 (2007) 191–285.
- [14] Y. Uchimura, M. Nakao, H. Saitoh, Generation of SUMO-1 modified proteins in *E. coli*: towards understanding the biochemistry/structural biology of the SUMO-1 pathway, *FEBS Lett.* 564 (2004) 85–90.
- [15] P. Romero, Z. Obradovic, X. Li, E.C. Garner, C.J. Brown, A.K. Dunker, Sequence complexity of disordered protein, *Proteins* 42 (2001) 38–48.
- [16] V.N. Uversky, What does it mean to be natively unfolded?, *Eur. J. Biochem.* 269 (2002) 2–12.
- [17] P.V. Konarev, V.V. Volkov, A.V. Sokolova, M.H. Koch, D. Svergun, PRIMUS – a Windows-PC based system for small-angle scattering data analysis, *J. Appl. Crystallogr.* 36 (2003) 1277–1282.
- [18] D.I. Svergun, Determination of the regularization parameter in indirect transform methods using perceptual criteria, *J. Appl. Crystallogr.* 25 (1992) 495–503.
- [19] D.I. Svergun, M.V. Petoukhov, M.H. Koch, Determination of domain structure of proteins from X-ray solution scattering, *Biophys. J.* 80 (2001) 2946–2953.
- [20] V.V. Volkov, D.I. Svergun, Uniqueness of ab initio shape determination in small-angle scattering, *J. Appl. Crystallogr.* 2003 (2003) 860–864.
- [21] J.M. Bourhis, V. Receveur-Brechot, M. Oglesbee, X. Zhang, M. Buccellato, H. Darbon, B. Canard, S. Finet, S. Longhi, The intrinsically disordered C-terminal domain of the measles virus nucleoprotein interacts with the C-terminal domain of the phosphoprotein via two distinct sites and remains predominantly unfolded, *Protein Sci.* 14 (2005) 1975–1992.
- [22] G.C. Bressan, J.C. Silva, J.C. Borges, D.O. Dos Passos, C.H. Ramos, I.L. Torriani, J. Kobarg, Human regulatory protein Ki-157 has characteristics of an intrinsically unstructured protein, *J. Proteome Res.* 7 (2008) 4465–4474.
- [23] M. Nardini, D. Svergun, P.V. Konarev, S. Spano, M. Fasano, C. Bracco, A. Pesce, A. Donadini, C. Cericola, F. Secundo, A. Luini, D. Corda, M. Bolognesi, The C-terminal domain of the transcriptional co-repressor CtBP is intrinsically unstructured, *Protein Sci.* 15 (2006) 1042–1050.
- [24] P. Bayer, A. Arndt, S. Metzger, R. Mahajan, F. Melchior, R. Jaenicke, J. Becker, Structure determination of the small ubiquitin-related modifier SUMO-1, *J. Mol. Biol.* 280 (1998) 275–286.
- [25] K.M. Campbell, A.R. Terrell, P.J. Laybourn, K.J. Lumb, Intrinsic structural disorder of the C-terminal activation domain from the bZIP transcription factor Fos, *Biochemistry* 39 (2000) 2708–2713.
- [26] M. Wells, H. Tidow, T.J. Rutherford, P. Markwick, M.R. Jensen, E. Mylonas, D.I. Svergun, M. Blackledge, A.R. Fersht, Structure of tumor suppressor p53 and its

- intrinsically disordered N-terminal transactivation domain, *Proc. Natl. Acad. Sci. USA* 105 (2008) 5762–5767.
- [27] M.K. Yoon, J. Shin, G. Choi, B.S. Choi, Intrinsically unstructured N-terminal domain of bZIP transcription factor HY5, *Proteins* 65 (2006) 856–866.
- [28] J. Liu, N.B. Perumal, C.J. Oldfield, E.W. Su, V.N. Uversky, A.K. Dunker, Intrinsic disorder in transcription factors, *Biochemistry* 45 (2006) 6873–6888.
- [29] Y. Minezaki, K. Homma, A.R. Kinjo, K. Nishikawa, Human transcription factors contain a high fraction of intrinsically disordered regions essential for transcriptional regulation, *J. Mol. Biol.* 359 (2006) 1137–1149.
- [30] K. Nakae, K. Nakajima, J. Inazawa, T. Kitaoka, T. Hirano, ERM, a PEA3 subfamily of Ets transcription factors, can cooperate with c-Jun, *J. Biol. Chem.* 270 (1995) 23795–23800.
- [31] J. Schneikert, H. Peterziel, P.A. Defossez, H. Klocker, Y. Launoit, A.C. Cato, Androgen receptor-Ets protein interaction is a novel mechanism for steroid hormone-mediated down-modulation of matrix metalloproteinase expression, *J. Biol. Chem.* 271 (1996) 23907–23913.
- [32] M. Pastorcic, H.K. Das, The C-terminal region of CHD3/ZFH interacts with the CIDD region of the Ets transcription factor ERM and represses transcription of the human presenilin 1 gene, *FEBS J.* 274 (2007) 1434–1448.
- [33] M. Pastorcic, H.K. Das, Analysis of transcriptional modulation of the presenilin 1 gene promoter by ZNF237, a candidate binding partner of the Ets transcription factor ERM, *Brain Res.* 1128 (2007) 21–32.
- [34] D. Baba, N. Maita, J.G. Jee, Y. Uchimura, H. Saitoh, K. Sugawara, F. Hanaoka, H. Tochio, H. Hiroaki, M. Shirakawa, Crystal structure of thymine DNA glycosylase conjugated to SUMO-1, *Nature* 435 (2005) 979–982.
- [35] M.S. Macauley, W.J. Errington, M. Scharpf, C.D. Mackereth, A.G. Blaszcak, B.J. Graves, L.P. McIntosh, Beads-on-a-string, characterization of ETS-1 sumoylated within its flexible N-terminal sequence, *J. Biol. Chem.* 281 (2006) 4164–4172.
- [36] M.S. Macauley, W.J. Errington, M. Okon, M. Scharpf, C.D. Mackereth, B.A. Schulman, L.P. McIntosh, Structural and dynamic independence of isopeptide-linked RanGAP1 and SUMO-1, *J. Biol. Chem.* 279 (2004) 49131–49137.
- [37] A. Pichler, P. Knipscheer, E. Oberhofer, W.J. van Dijk, R. Korner, J.V. Olsen, S. Jentsch, F. Melchior, T.K. Sixma, SUMO modification of the ubiquitin-conjugating enzyme E2-25K, *Nat. Struct. Mol. Biol.* 12 (2005) 264–269.
- [38] Y. Tateishi, M. Ariyoshi, R. Igarashi, H. Hara, K. Mizuguchi, A. Seto, A. Nakai, T. Kokubo, H. Tochio, M. Shirakawa, Molecular basis for SUMOylation-dependent regulation of DNA binding activity of heat shock factor 2, *J. Biol. Chem.* 284 (2009) 2435–2447.
- [39] J. Kim, S. Sharma, Y. Li, E. Cobos, J.J. Palvimo, S.C. Williams, Repression and coactivation of CCAAT/enhancer-binding protein epsilon by sumoylation and protein inhibitor of activated STAT proteins, *J. Biol. Chem.* 280 (2005) 12246–12254.